Supplementary Information is available on *Nature*'s World-Wide Web site (http://www.nature.com) or as paper copy from the London editorial office of *Nature*.

Acknowledgements. The current development of the Northern Hemisphere densitometric network is funded by the Swiss National Science Foundation (F.H.S.) and the European Community under ADVANCE-10K (K.R.B.). P.D.J. is supported by the US Department of Energy, and T.J.O. by NERC. We thank E. Cook, T. Crowley, M. Free, V. Morgan, E. Mosley-Thompson, C. Newhall, F. Oldfield, A. Robock and S. Self for advice and data.

Correspondence and requests for materials should be addressed to K.R.B. (e-mail: k.briffa@uea.ac.uk).

Global influence of the AD1600 eruption of Huaynaputina, Peru

Shanaka L. de Silva* & Gregory A. Zielinski†

** Department of Geography, Geology, and Anthropology, Indiana State University, Terre Haute, Indiana 47809, USA*

† Climate Change Research Center, University of New Hampshire, Durham, New Hampshire 03824-3525, USA

It has long been estabished that gas and fine ash from large equatorial explosive eruptions can spread globally, and that the sulphuric acid that is consequently produced in the stratosphere can cause a small, but statistically significant, cooling of global temperatures[1,2]. Central to revealing the ancient volcano–climate connection have been studies linking single eruptions to features of climate-proxy records such as found in ice-core[3–5] and tree-ring[6–8] chronologies. Such records also suggest that the known inventory of eruptions is incomplete, and that the climatic significance of unreported or poorly understood eruptions remains to be revealed. The AD1600 eruption of Huaynaputina, in southern Peru, has been speculated to be one of the largest eruptions of the past 500 years; acidity spikes from Greenland and Antarctica ice[3–5], tree-ring chronologies[6–8], along with records of atmospheric perturbations in early seventeenth-century Europe and China[9,10], implicate an eruption of similar or greater magnitude than that of Krakatau in 1883. Here we use tephra deposits to estimate the volume of the AD1600 Huaynaputina eruption, revealing that it was indeed one of the largest eruptions in historic times. The chemical characteristics of the glass from juvenile tephra allow a firm cause–effect link to be established with glass from the Antarctic ice, and thus improve on estimates of the stratospheric loading of the eruption.

Volcan Huaynaputina, located at 16° 35′ S, 70° 52′ W in the Moquegua region of southern Peru (Fig. 1), consists of three craters situated at 4,500 m within the amphitheatre of an ancient strato-volcano. A compilation of historical and parochial literature[11] reveals that the volcano formed during an eruption that began on 19 February 1600 and continued until 5 March. The fall deposit covered an area of at least 300,000 km^2 in southern and west central Peru, western Bolivia and north Chile (Fig. 1). Ashfall was reported on the major cities of Lima, La Paz (Bolivia) and Arica (Chile) as well as on a ship 1,000 km to the west[11]. The fall seems to have been distributed predominantly to the west and north. Local proximal pyroclastic flows and secondary mass flows were insignificant in volume. This large plinian eruption destroyed local communities with a loss of over 1,000 lives and caused considerable damage to the major cities of Arequipa and Moquegua. The loss of farmland, crops, livestock, vineyards, and water resources compounded the significant economic burden on this region. The whole socio-economic infrastructure of a large part of Peru, and maybe that of

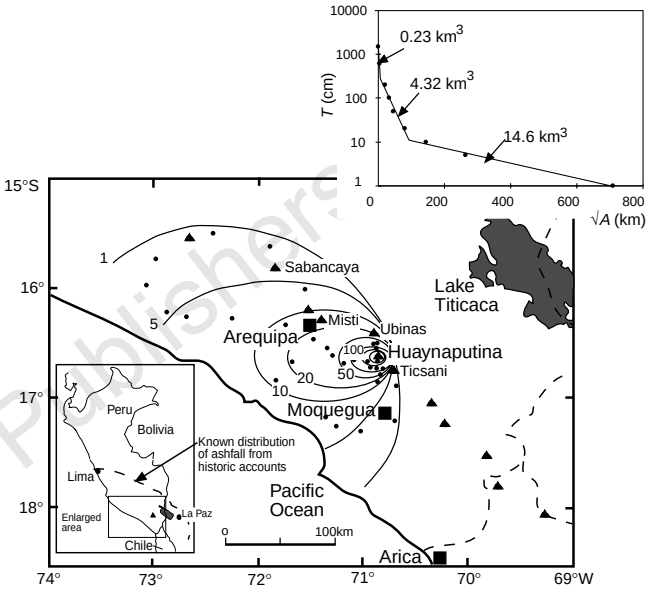

Figure 1 Isopach map of Huaynaputina tephra deposit showing the strong westerly distribution of the deposit. Black triangles are volcanoes of the modern volcanic arc and the most recently active are labelled; small dots are data points. Volcan Ticsani, the site of a similar but smaller eruption to Huaynaputina, is also shown. Values associated with contours are in centimetres; two innermost contours not labelled are 200 and 600 cm respectively, and the 1,500 cm contour is covered by the symbol for the volcano. The graph in the upper right corner shows a plot of thickness (T) on a logarithmic scale against the square root of isopach area[31,32]. The thickness data are described by three line segments that define a typical exponential profile. Integration beneath the line segments with respect to area, following the method of Fierstein and Nathenson[32], and removing the volume achieved by extrapolating the data to zero thickness[31], yields the volumes noted for each segment and the minimum volume of tephra of 19.2 km^3. Negative error in this estimate is limited to measurement and area estimation errors and is ~10% for this data set. Positive errors far outweigh this, as discussed in the text. Inset (bottom left) shows the known distribution of the fall from the AD1600 eruption (broken line) based on a compilation of parochial and historical accounts[11]. The box in the inset shows the area covered in the larger map. Note that our data cover only a small portion of the known distribution of the AD1600 tephra fall, albeit along the main axis. As most of the distal tephra has been lost, a considerable volume of distal tephra cannot be measured.

Table 1 Main oxide composition of individual juvenile clasts and volcanic glass from the Huaynaputina eruption compared with tephra from the early 1600s of the Antarctica and Greenland ice cores

	Huaynaputina bulk rock* (21 samples)	Huaynaputina glass* (n = 103; 6 samples)	Huaynaputina glass† (n = 7)	South Pole glass† (n = 16)	GISP2 glass* (n = 16)
SiO_2	65.16 ± 0.70	72.82 ± 0.68	75.76 ± 0.53	72.92 ± 2.04	62.1 ± 4.7
TiO_2	0.58 ± 0.03	0.26 ± 0.20	0.27 ± 0.06	0.34 ± 0.20	1.1 ± 0.5
Al_2O_3	16.68 ± 0.40	15.20 ± 1.21	13.85 ± 0.15	13.98 ± 0.91	16.2 ± 2.5
FeO	3.97 ± 0.17	1.31 ± 0.25	1.10 ± 0.14	1.37 ± 0.28	8.2 ± 3.5
MgO	1.78 ± 0.12	0.30 ± 0.13	0.27 ± 0.14	0.44 ± 0.20	1.9 ± 1.0
CaO	3.88 ± 0.17	1.61 ± 0.32	1.22 ± 0.07	1.41 ± 0.35	3.9 ± 1.7
Na_2O	4.57 ± 0.09	4.53 ± 0.34	3.43 ± 0.24	4.12 ± 0.73	4.0 ± 1.1
K_2O	2.79 ± 0.15	3.82 ± 0.18	3.89 ± 0.15	3.76 ± 0.28	2.5 ± 0.9

Errors are 1σ. n = number of individual analyses. Bulk rock analyses are of juvenile clasts from proximal and medial locations.
* This study.
† From ref. 16.

Table 2 Climate proxy data and atmospheric phenomena indicative of explosive volcanism in the earliest 1600s with known eruptions AD 1600–04

Ice core data

Location	Signal type/characteristics	Year of signal with error	Total volcanic flux kg km^{-2} (time)	Stratospheric mass loading (Mt)	
				Huaynaputina	Tambora
Greenland					
GISP2[4]	SO_4^{2-} doublet	1603–04 (±2)	36 (2 yr)	87	86
GRIP[21]	ECM doublet	1601–02 (±1)	36 (2.3 yr)	52	38
	SO_4^{2-} doublet	1601–02 (±1)	54 (2 yr)	78	101
Crete[3]	ECM doublet	1601–02 (±1)	61 (2 yr)	50	150
Antarctica					
South Pole[5]	SO_4^{2-} peak	1601 (±5)	22.5 (3–4 yr)	100	307
Siple Station[22]	SO_4^{2-} peak	1599 (±2)	34 (~4 yr)	n.d.	n.d.
Dyer Plateau[22]	SO_4^{2-} peak	1599 (±2)	30 (~4 yr)	n.d.	n.d.

Tree ring

Phenomenon	Location	Year	Comment
Narrow ring widths	Fennoscandia	1601	Calibrated to fourth coldest summer over past 1,500 years[23]
	Western USA	1601	Calibrated to coldest summer in most of western North America over past 400 years[24]
	Northern Hemisphere	1601	Calibrated to coldest summer over past 600 years[7,8]
	Sierra Nevada	1601	Cold summer[25]
Frost rings	Western USA	1601	Below freezing temperatures during growing season[6]
Light rings	Upper tree line, Quebec	1601 and 1603	Cold temperatures near end of growing season[26]

Atmospheric phenomena

Location	Comments
Scandinavia	Sun dimmed by constant haze in 1601 (ref. 9)
Central Europe	All through 1601 until the end of July 1602, Sun and Moon "reddish, faint and lacked brilliance". These phenomena led to minimum total (1601–04) dust veil index (DVI) estimate of 1,000 by comparison with phenomena associated with 1883 Krakatau and 1783 Laki eruptions (ref. 9).
Iceland	Summer of 1601, Sun pale and sunlight so faint that shadows not cast. Sky appeared cloudy and pale even when no clouds present. Winter of 1601–02 extremely severe (G. Larsen, personal communication, after ref. 27).
China	1603, red and dim Suns; 1604, large sunspots (ref. 10).
Graz, Austria	Darkened partial lunar eclipse in December 1601 implies a Northern Hemisphere average optical depth of 0.10, comparable to El Chichón and Agung, although if the dimness of the December 1601 partial eclipse was from Huaynaputina aerosols, then the 0.10 optical depth would not have been the maximum optical depth, but an optical depth following almost two years of aerosol loss from the stratosphere (R. Keen, personal communication after refs 28, 29).

Potential source eruptions (ref. 30 unless stated otherwise)

Volcano (latitude) tephra	Date of eruption	VEI	Volume (km^3)
Asama (Japan, 36° N)	January 1600	3?	?
Huaynaputina (Peru, 17° S) (this work)	February 1600	6	>19
Suwanose-Jima (Ryuku Is., 30° N)	1600 (year questionable)	4+	?
Iwaki (Japan, 41° N)	February 1604	3?	?

n.d., not determined, but considering that flux values are slightly higher than the South Pole values, loading estimates would be similar to or slightly above the 100 Mt estimate.

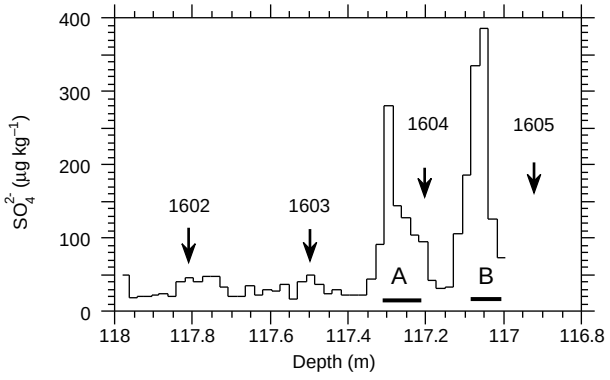

◀ **Figure 2** Subseasonal record of sulphate concentrations in the GISP2 ice core for the period AD 1601–05. Arrows denote mid-summer for the year shown. Maximum dating error for this period is only ~2 years. It is believed, from correlation with the other ice cores, that the ages shown might be 1 or 2 years too young, although the red Suns observed in China in 1603 (Table 2) indicate that there still was a significant stratospheric aerosol loading in that year. Deposition of those aerosols on Greenland could easily have been in 1604. Even if the two sulphate spikes correspond to 1601/1602 and 1602/1603, these are ages within the error of the GSIP2 dating shown on the figure. Flux of the volcanic sulphate component of the record is 13 kg km^{-2} per 0.5 year for peak A and 21 kg km^{-2} per 0.5 yr for peak B from the detailed (~14 samples yr^{-1}) results presented here. Total volcanic flux of 34 kg km^{-2} per 2 yr agrees well with the 36 kg km^{-2} per 2 yr obtained from the original biyearly sampling done on the GISP2 core[4] and given in Table 1. Total volcanic sulphate flux is determined by the sum of the products of concentration, measured ice density and length for each sample. Volcanic sulphate concentration is the total concentration minus average background levels. Sea-salt sulphate was removed from the calculations. A and B also indicate the length of sections of ice filtered in an attempt to locate and identify volcanic glass with a scanning electron microscope and electron microprobe. Figure modified from ref. 4.

Bolivia and Chile, was devastated by the eruption. A full recovery of the economy took almost 150 years (ref. 11).

We calculated new estimates of the volume erupted on the basis of field measurements of present-day tephra thicknesses and the construction of an isopach map (Fig. 1). From this a minimum erupted tephra volume of ~19.2 km^3 was calculated. Preliminary measurements of bulk tephra densities yield a weighted average density of ~1,200 $kg\,m^{-3}$, which yields a minimum dense rock equivalent (DRE) or magma equivalent volume of ~9.6 km^3. This is the first and only volume estimate based on field measurements for this eruption. The true volume of the eruption might be considerably larger. First, our estimate does not include distal tephra outside the mapped isopachs. Second, our measurements cover only a portion of the area of the fall deposit, albeit along the main axis of the deposit (Fig. 1). Last, historical and anecdotal information[11] clearly report greater thicknesses of tephra deposition than we find in the field today. For instance, during the first 24 h alone, over 20 cm of sand-sized tephra fell in Arequipa. Over 1 m of ash was reported in regions to the north and west of Arequipa after the eruption; today we find a maximum of 10 cm. Even allowing for compaction of distal ash, this still suggests that a considerable amount of the tephra has been lost, most obviously to deflation, mass wasting, and agriculture. Speculation about true volume aside, our minimum estimate for the tephra deposit of 19.2 km^3 firmly establishes this eruption as a magnitude 6 on the Volcanic Explosivity Index (VEI (ref. 12)). This alone places this eruption firmly in the realms of the largest historic eruptions such as Krakatau in 1883 (ref. 13) (18 km^3 tephra; VEI ~6), Novarupta (Katmai) in 1912 (ref. 14) (~20–25 km^3 tephra; VEI ~6) and Mt Pinatubo in 1991 (ref. 15) (10 km^3 tephra; VEI 6).

New geochemical data on the products of the eruption now allow us to establish a much firmer link between this eruption and the volcanic glass found in the ice-core record. These data reveal that the magma of the AD1600 eruption was a monotonous calc-alkaline dacite (Table 1). The juvenile clasts of non-expanded to moderately expanded dacite contain ~30–35 vol.% phenocrysts of plagioclase > amphibole > oxides > apatite set in a matrix of fresh glass. Huaynaputina magmatic compositions are distinct from other late Cenozoic to recent volcanics of similar composition in this region; of particular note here is that the ratio of Na_2O to K_2O is greater than 1 for the Huaynaputina magma (Table 1). Our data for the glass reveal this same distinctive character (Table 1) and are a much closer match to the analyses of volcanic glass in the South Pole ice core than presented in previous studies[16]. These data provide the strongest support yet for the presence of volcanic glass from Huaynaputina in the South Pole ice core and thus the climatic impact of the eruption might be better delineated.

Climate-proxy data (Table 2) indicate that the earliest part of the seventeenth century and especially the summer of 1601 was the coldest of the past 600 years throughout much of the Northern Hemisphere and among the coldest of the past 1,500 years in Fennoscandia. High levels of H_2SO_4 found in ice-core layers dated to 1599–1604 (with dating error) from both polar regions, together with observed atmospheric phenomena (Table 2), strongly suggest that volcanism, and presumably an equatorial eruption such as Huaynaputina, had some role in forcing that cooling[17]. In fact, the mean estimate of the stratospheric loading of H_2SO_4 based on the Greenland ice core record is 67 ± 16 Mt or twice that estimated for the Mt Pinatubo eruption in 1991 (~30 Mt; ref. 18). The 67 Mt estimate is ~78% of the stratospheric loading estimated for the 1815 Tambora eruption from data from these same ice cores (Table 2). The only estimate for Huaynaputina from Antarctica is 100 Mt H_2SO_4 (Table 2). These values are substantial enough to force climate cooling.

How much of this stratospheric loading and subsequent cooling can confidently be attributed to Huaynaputina? On the basis of the strong evidence for Huaynaputina glass in the South Pole core, the 100 Mt estimate can reasonably be related entirely to the Huaynaputina eruption.

The Greenland data are more problematic because the volcanic signal occurs as a distinct doublet peak in Northern-Hemisphere ice cores, and we cannot link the earlier peak of the GISP2 core doublet (Fig. 2) to Huaynaputina because the glass compositions do not match (Table 1). This implicates another eruption as the main source of the sulphate; glass from Asama, Japan[19], do not match either, so the most likely source is either the Suwanose-Jima eruption (Table 2) or a previously undocumented eruption originating in the Northern Hemisphere. Higher total volcanic flux values in signals from the early 1600s in the Greenland ice cores relative to Antarctica, particularly given the 17° S location of Huaynaputina, would probably result from an eruption directly upwind from Greenland. This notwithstanding, it is reasonable to argue that ash particles are less likely than aerosols to be transported interhemispherically from a tropical eruption such as Huaynaputina: the lack of ash particles does not categorically negate a role for this eruption. We therefore make the conservative assumption that the younger sulphate spike in the GISP2 core (B in Fig. 2) is from Huaynaputina. This yields a volcanic sulphate flux of 21 $kg\,km^{-2}$ per 0.5 yr from the GISP2 core, which translates to a stratospheric mass loading estimate of ~50 Mt (ref. 4) or two-thirds of the total GISP2 volcanic signal over these two years. If a similar proportion of Huaynaputina acid is found in the total signals for the other Greenland cores, then the mean Northern Hemisphere loading for Huaynaputina would be ~42 ± 10 Mt or almost 50% greater loading than Pinatubo, but only one-half of the Tambora loading for the Northern Hemisphere. A composite estimate of stratospheric loading from Greenland snow records for the equatorial El Chichón eruption agreed well with satellite estimates[20]; thus our estimate of the stratospheric loading for the Huaynaputina eruption derived from this series of Greenland ice cores should be reliable. The 100 Mt loading estimate for the Southern Hemisphere, based on the South Pole core (Table 2), might be a reflection of the southern equatorial location of the volcano and the greater distribution of aerosols to southern polar regions. These two hemispheric estimates yield a global average of ~70 Mt H_2SO_4 for the Huaynaputina eruption. This is only 35% of the ~200 Mt (global average) estimated for Tambora, the greatest sulphur-producing eruption of at least the past ~750 years. Nevertheless, these data indicate that the Huaynaputina eruption was very capable of forcing global climate, and its atmospheric perturbation was not only far greater than any eruption in the twentieth century, it is also one of the greatest of historical time. □

Received 7 July 1997; accepted 10 April 1998.

1. Cadle, R. D., Kiang, C. S. & Louis, J. F. The global scale dispersion of the eruption clouds from major volcanic eruptions. *J. Geophys. Res.* **81,** 3125–3132 (1976).
2. Mass, C. F. & Portman, D. A. Major volcanic eruptions and climate: a critical evaluation. *J. Clim.* **2,** 566–593 (1989).
3. Hammer, C. U., Clausen, H. B. & Dansgaard, W. Greenland ice sheet evidence of post-glacial volcanism and its climatic impact. *Nature* **288,** 230–235 (1980).
4. Zielinski, G. A. Stratospheric loading and optical depth estimates of explosive volcanism over the last 2100 years derived from the GISP2 Greenland ice core. *J. Geophys. Res.* **100,** 20937–20955 (1995).
5. Delmas, R. J., Kirchner, S., Palais, J. M. & Petit, J. R. 1000 years of explosive volcanism recorded at the South Pole. *Tellus* **B44,** 335–350 (1992).
6. LaMarche, V. C. & Hirschboeck, K. K. Frost rings in trees as records of major volcanic eruptions. *Nature* **307,** 121–126 (1984).
7. Jones, P. D., Briffa, K. R. & Schweingruber, F. H. Tree-ring evidence of the widespread effects of explosive volcanic eruptions. *Geophys. Res. Lett.* **22,** 1333–1336 (1995).
8. Briffa, K. R., Jones, P. D., Schweingruber, F. H. & Osborn, T. J. Influence of volcanic eruptions on Northern Hemisphere summer temperatures over 600 years. *Nature* **393,** 450–455 (1998).
9. Lamb, H. H. Volcanic dust in the atmosphere; with a chronology and assessment of its meteorological significance. *Phil. Trans. R. Soc. Lond. A* **266,** 425–533 (1970).
10. Scuderi, L. A. Oriental sunspot observations and volcanism. *Q. J. R. Astron. Soc.* **31,** 109–120 (1990).
11. de Silva S. L., Alzueta, J. & Salas, G. in *Volcanic Disasters in Human Antiquity* (eds Heiken, G. & McCoy, F.) (Geol. Soc. Am. Spec. Paper, in the press).
12. Newhall, C. & Self, S. The volcanic explosivity index (VEI): an estimate of explosive magnitude for historical volcanism. *J. Geophys. Res.* **87,** 1231–1238 (1982).
13. Simkin, T. & Fiske, R. *Krakatau 1883; the Volcanic Eruption and its Effects* (Smithsonian Inst., Washington DC, 1983).
14. Hildreth, W. New perspectives on the eruption of 1912 Valley of Ten Thousand Smokes, Katmai National Park, Alaska. *Bull. Volcanol.* **49,** 680–693 (1987).
15. Scott, W. E. *et al.* in *Fire Mud: Eruptions and Lahars of Mount Pinatubo, Philippines* (eds Newhall, C. G.

& Punongbayan, R. S.) 545–571 (Univ. Washington Press, Seattle, 1996).
16. Palais, J. M., Kirchner, S. & Delmas, R. J. Identification of some global volcanic horizons by major element analysis of fine ash in Antarctic ice. *Ann. Glaciol.* **14,** 216–220 (1990).
17. Pyle, D. M. On the 'climate effectiveness' of volcanic eruptions. *Quat. Res.* **37,** 125–129 (1992).
18. McCormick, M. P., Thomason, L. W. & Trepte, C. R. Atmospheric effects of the Mt Pinatubo eruption. *Nature* **373,** 399–404 (1995).
19. Zielinski, G. A. *et al.* Climatic impact of the AD 1783 eruption of Asama (Japan) was minimal: evidence from the GISP2 ice core. *Geophys. Res. Lett.* **21,** 2365–2368 (1994).
20. Zielinski, G. A. *et al.* Assessment of the record of the 1982 El Chichón eruption as preserved in Greenland snow. *J. Geophys. Res.* **102,** 30031–30045 (1997).
21. Clausen, H. B. *et al.* A comparison of the volcanic records over the past 4000 years from the Greenland ice core project and Dye 3 Greenland ice cores. *J. Geophys. Res.* **102,** 26707–26723 (1997).
22. Cole-Dai, J., Mosley-Thompson, E. & Thompson, L. Annually resolved southern hemisphere volcanic history from two Antarctic ice cores. *J. Geophys. Res.* **102,** 16761–16771 (1997).
23. Briffa, K. R. *et al.* Fennoscandian summers from AD 500: temperature changes on short and long timescales. *Clim. Dyn.* **7,** 111–119 (1992).
24. Briffa, K. R., Jones, P. D. & Schweingruber, F. H. Tree-ring density reconstructions of summer temperature patterns across western North America since 1600. *J. Clim.* **5,** 735–754 (1992).
25. Scuderi, L. A. Tree ring evidence for climatically effective volcanic eruptions. *Quat. Res.* **34,** 67–86 (1990).
26. Filion, L., Payette, S., Gauthier, L. & Boutin, Y. Light rings in subarctic conifers as a dendrochronological tool. *Quat. Res.* **26,** 272–279 (1986).
27. Anonymous *Annáler* **6,** 493–494 (1400–1800).
28. Frisch, C. (ed.) *Joannis Kepleris Astronomi Opera Omnia* **2/3** (1856–1871).
29. Keen, R. A. Volcanic aerosols and lunar eclipses. *Science* **222,** 1011–1013 (1983).
30. Simkin, T. & Siebert, L. *Volcanoes of the World* 2nd edn (Geoscience Press, Tucson, 1994).
31. Pyle, D. M. The thickness, volume, and grainsize of trephra fall deposits. *Bull. Volcanol.* **51,** 1–15 (1989); Assessment of the minimum volume of tephra fall deposits. *J. Volcanol. Geotherm. Res.* **69,** 379–382 (1995).
32. Fierstein, J. & Nathenson, M. Another look at the calculation of fallout tephra volume. *Bull. Volcanol.* **54,** 156–167 (1991).

Acknowledgements. We thank G. Salas, P. Francis, S. Self and the Instituto Geofisico de Peru, particularly the late M. Chang, for their collaboration on this project; P. Mayewski, L. D. Meeker, S. Whitlow and M. Twickler for their work in producing the initial sulphate time series of the GISP2 ice core; M. Germani and J. Palais for their help with the GISP2 tephra studies; J. Fierstein, M. Nathenson and N. Adams for help and discussions about the volume estimates; the members of the GISP2 community for work in developing the chronology of the core; and the Science Management Office, Polar Ice Coring Office and 109th Air National Guard for logistical support. Funding for this work has come from Indiana State University, and the National Science Foundation Petrology and Geochemistry Program, Office of Polar Programs (GISP2 work), and Atmospheric Sciences Program. The manuscript has benefited considerably from thorough reviews by D. Pyle and P. Allard.

Correspondence and requests for materials should be addressed to S.L.d.S. (e-mail: gesilva@scifac.indstate.edu).

A one-million-year-old *Homo* cranium from the Danakil (Afar) Depression of Eritrea

Ernesto Abbate*, Andrea Albianelli*, Augusto Azzaroli†, Marco Benvenuti*, Berhane Tesfamariam‡, Piero Bruni*, Nicola Cipriani*, Ronald J. Clarke§, Giovanni Ficcarelli*, Roberto Macchiarelli‖, Giovanni Napoleone*, Mauro Papini*, Lorenzo Rook*, Mario Sagri*, Tewelde Medhin Tecle¶, Danilo Torre† & Igor Villa#

* *Dipartimento di Scienze della Terra, Università di Firenze, 50121 Firenze, Italy*
† *Museo di Storia Naturale, Sezione di Geologia e Paleontologia, Università di Firenze, 50121 Firenze, Italy*
‡ *Eritrea National Museum, Asmara, Eritrea*
§ *Palaeo-Anthropology Research Unit, Department of Anatomical Sciences, University of the Witwatersrand Medical School, Johannesburg 2193, South Africa*
‖ *Museo Nazionale Preistorico Etnografico 'L. Pigorini', Sezione di Antropologia, 00144 Roma, Italy*
¶ *Ministry of Energy, Water and Mineral Resources, Department of Mines, Asmara, Eritrea*
# *Mineralogisches Institut, Abteilung für Isotopengeologie, Universität Bern, Switzerland*

One of the most contentious topics in the study of human evolution is that of the time, place and mode of origin of *Homo sapiens*[1–3]. The discovery in the Northern Danakil (Afar) Depression, Eritrea, of a well-preserved *Homo* cranium with a mixture of characters typical of *H. erectus* and *H. sapiens* contributes significantly to this debate. The cranium was found in a succession of fluvio-deltaic and lacustrine deposits and is associated with a rich mammalian fauna of early to early-middle Pleistocene age. A magnetostratigraphic survey indicates two reversed and two normal magnetozones. The layer in which the cranium was found is near the top of the lower normal magnetozone, which is identified as the Jaramillo subchron. Consequently, the human remains can be dated at ~1 million years before present.

The cranium, two incisors and two pelvic fragments were recovered between 1995 and 1997 near the village of Buia, Eritrea, about 100 km south-south-east of Massawa in the Danakil Formation, which is more than 1,000 m thick. This unit, also known as the Red Series[4,5], crops out extensively in the Danakil Depression, a belt of pronounced lithospheric extension at the intersection of the Red Sea, the Gulf of Aden, and the East African rift systems[6] (Fig. 1). It consists mainly of siliciclastic continental deposits with intercalations of lava flows and tuff beds at different levels. A Miocene to Pleistocene age is commonly assumed[4,5,7,8], and from a chronological and palaeo-environmental point of view, this formation can be correlated with the well-known hominid-bearing Awash Group in Ethiopia[9].

We examined the upper 500-m-thick portion of the Danakil Formation that is composed of grey to whitish clayey silts and sands with small amounts of marls laid down in fluvio-deltaic and lacustrine environments (Fig. 2).

Ash layers containing biotite have been found in the lower portion of the section. An initial attempt to date a biotite bulk separate by $^{39}Ar/^{40}Ar$ failed because of xenocrystic contamination.

As well as freshwater gastropod and fish remains, a large amount of fossil bones were found along the entire Buia section, and five mammal-rich levels have been identified (Fig. 2). The third level from the base yielded *Homo* remains consisting of a nearly complete and undeformed adult cranium (UA 31) (Fig. 3), two pelvic fragments (UA 173), and two permanent lower incisors (UA 222 and UA 369).

In the *Homo*-bearing outcrop, silts and clays alternate with sands. The cranium and pelvic fragments come from the upper part of a layer of laminated silty clays 1.4 m thick. The UA 369 incisor was

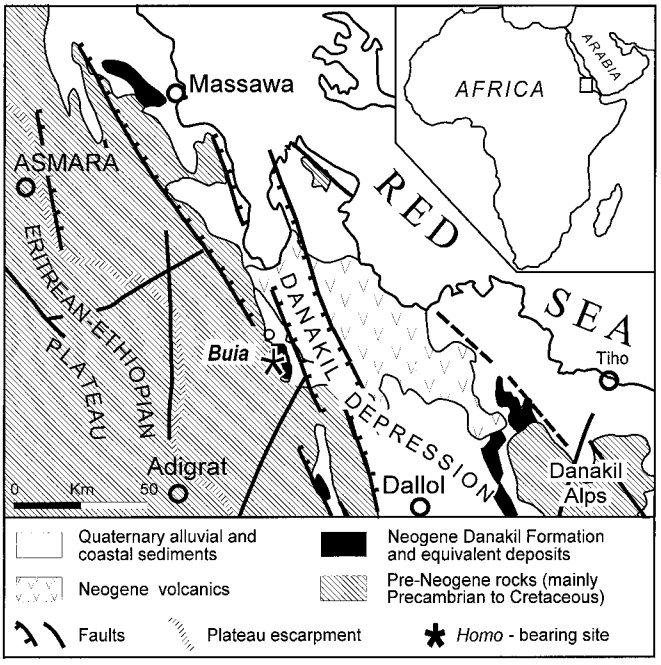

Figure 1 Simplified geology of the Northern Danakil Depression between the Eritrean-Ethiopian plateau and the Southern Red Sea. The palaeo-anthropological site near Buia is indicated by an asterisk.